RELIABILITY ASSESSMENT OF SOLDER JOINT INTERCONNECTS OF BGA PACKAGE-MEGTRON SERIES UNDER POWER CYCLING

by

MAHESH PALLAPOTHU

Presented to the Faculty of the Graduate School of
The University of Texas at Arlington in Partial Fulfillment
of the Requirements
for the Degree of

MASTER OF SCIENCE IN MECHANICAL ENGINEERING

THE UNIVERSITY OF TEXAS AT ARLINGTON
December 2017

Acknowledgements

I would like to thank my advisor and mentor, Dr. Dereje Agonafer for giving me a great opportunity to join his team and providing me continuous guidance. It was an honor and I feel proud to have worked with him.

I want to express my sincere gratitude to Dr. A. Haji-Sheikh and Dr. Andrey Beyle for being my committee members and evaluating my thesis work.

I would like to extend my thanks to all the members of EMNSPC team. A special thanks to Mugdha Chaudhari, Pavan Rajmane, Unique Rahangdale, Aniruddha Doiphode and Abel Misrak for helping me through my thesis and giving me valuable suggestions. It was great working with all of you.

I am always grateful to my parents for providing me with all the facilities and support I needed to work successfully towards the completion of my master's degree.

November 9, 2017

Abstract

RELIABILITY ASSESSMENT OF SOLDER JOINT INTERCONNECTS OF BGA PACKAGE-MEGTRON SERIES UNDER POWER CYCLING

MAHESH PALLAPOTHU, MS

The University of Texas at Arlington, 2017

Supervising Professor: Dereje Agonafer

Solder joints interconnects are the second level assembly in surface mount interconnection technology. Mismatch in Coefficient of thermal expansion (CTE) between package and substrate or PCB creates failure in solder joints such as excessive warpage, low-k dielectric layer cracking, solder mask cracking and bump cracking. Conventional accelerated thermal cycling tests are performed to evaluate the Solder Joint Reliability (SJR). But, in everyday application, the package is subjected to Power cycling. Power cycling is the phenomenon where the package experiences non-uniform temperature distribution in the package with the chip as an internal heat generating source when an electronic device is turned on and off several times. This induces thermal stresses and deforms the package. High frequency laminates offer better fatigue life when compared with the traditional FR-4 material. In addition to the fatigue life they also possess properties like good impedance control, low moisture absorption capacity and improved thermal management. In this study, maximum accumulated plastic work per cycle is used as a parameter to estimate the life of the package in number of cycles it takes for failure at the solder joint interconnects. The reliability of the solder joint interconnects of a BGA package on various Megtron series boards is assessed and compared with FR-4 board under power cycling.

Table of Contents

List Of Illustrations

List of Tables

Chapter 1

INTRODUCTION

1.1 Printed Circuit Boards

Before the invention of the printed circuit boards, the electronic components in a circuit are interconnected using extremely bulky and unreliable designs which consisted of large sockets. The concept of miniaturization was hard to imagine. The Printed Circuit Board (PCB) directly addressed this issue. It mechanically supports and electrically connects the electronic components using conductive tracks, pads and other features etched from copper sheets laminated onto a non-conductive substrate. The PCB's may be classified into different types based on the number of layers- single, double and multi layers. The etched copper layers, which are the conductors, are connected between the different layers of a PCB with plated-throughs called vias. When compared with the single or double-sided PCB a multi-layered PCB have its several advantages like high assembly density, increased flexibility, easier incorporation controlled impedance features, EMI shielding through careful placement of power and ground layers, reduces the need for interconnection wiring harness which in turn reduces the overall weight.

FR-4 glass epoxy is the most common and primary insulating substrate used in the production of the PCB. A thin copper foil is laminated on both sides of the FR-4 layer. The etched copper layers are incorporated between the FR-4 layers which from the circuitry interconnections. The cross-section of a multi layered PCB is shown in the figure 1.1.

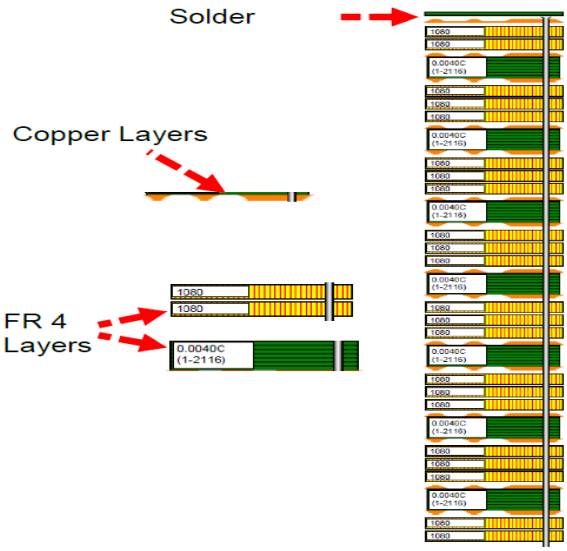

Figure 1.1: Cross-section of a 16 layered PCB

1.2 High Frequency Laminates

The conventional FR-4 laminate may not provide the high frequency performance needed for an application. Therefore, there is a need to explore new materials to obtain the desired reliability. Panasonic Megtron 6, Nelco N4000-13, Rogers RT/duroid are few high frequency laminates. These materials have low dielectric constant (Dk) and loss tangent and provide improved electrical performance, impedance control, thermal management, and low moisture absorption capacity.

Megtron 6 is advanced material designed for high-frequency applications which have a low dielectric constant, dissipation factor, high heat resistance, excellent through-hole reliability which is 5 times better that the conventional FR-4 material. The typical application of Megtron 6 are high-speed network equipment, IC testers and high frequency measuring instruments. Megtron 6 board is shown in the figure 1.2

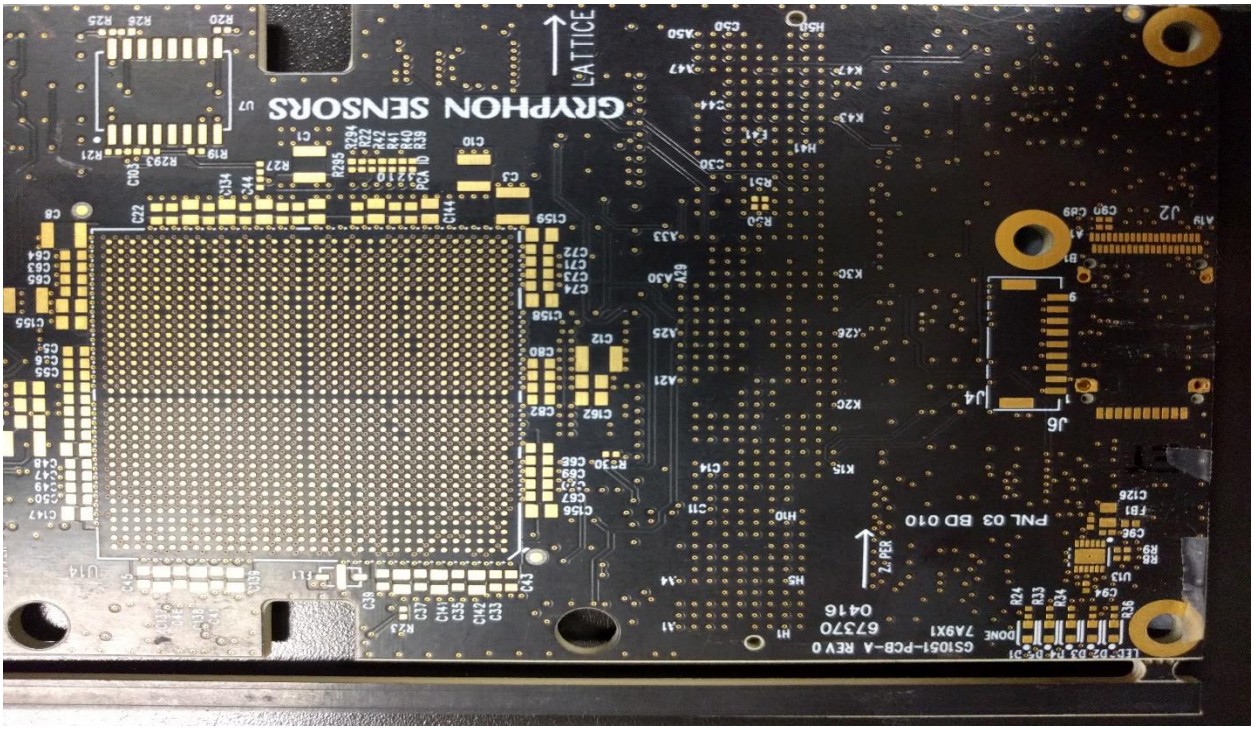

Figure 1.2: Megtron 6 board used for study

1.3 Ball Grid Array (BGA) Packages

Ball grid array (BGA) is a common surface mount package derived from a pin grid array (PIN) technology. It uses a grid of solder balls or leads to conduct electrical signals from the integrated circuit board. Instead of pins like the PGA, the BGA uses solder balls that are placed on the PCB. A typical BGA package is shown in the figure 1.3. The BGA packages can provide more interconnection where the whole bottom surface of the device is used, instead of just the perimeter, thus offering high density. The lower thermal resistance offered between the package and the PCB allows the heat generated by the integrated circuit inside the package to flow more easily to the PCB, preventing the chip from overheating. The BGA package also offers the advantage of low inductance due to short distance between the package and the PCB, which prevents the unwanted distortion of signals in high-speed electronic circuits, thus enhancing the electrical performance.

Figure 1.3: Ball Grid Array Package (BGA)

There are different types of BGA packages. They are:

- *CABGA*: Chip Array Ball Grid Array
- *CTBGA*: Thin Chip Array Ball Grid Array
- *CVBGA*: Very Thin Chip Array Ball Grid Array
- *DSBGA*: Die-Size Ball Grid Array
- *FBGA*: Fine Ball Grid Array based on *ball grid array*
- *FCBGA*: Flip Chip Ball Grid Array
- *LBGA*: Low-profile Ball Grid Array

- *LFBGA*: Low-profile Fine-pitch Ball Grid Array
- *MBGA*: Micro Ball Grid Array
- *MCM-PBGA*: Multi-Chip Module Plastic Ball Grid Array
- *PBGA*: Plastic Ball Grid Array
- *Super BGA (SBGA)*: Super Ball Grid Array
- *TABGA*: Tape Array BGA
- *TBGA*: Thin BGA
- *TEPBGA*: Thermally Enhanced Plastic Ball Grid Array
- *TFBGA* or Thin and Fine Ball Grid Array
- *UFBGA* and *UBGA* and Ultra Fine Ball Grid Array based on pitch ball grid array.
- *VFBGA*: Very Fine Pitch Ball Grid Array
- *WFBGA*: Very Very Thin Profile Fine Pitch Ball Grid Array

The BGA package used in this study is the Flip Chip Ball Grid Array Package (FCBGA). The flip chip technology differs from the wire-bonded package in a way that the interconnection between the die and carrier occurs using a conductive bump or die attach placed directly on the die surface. This surface is flipped and connected to the carrier directly. The advantages of a flip chip interconnection are the assembly is much smaller than a traditional carrier based system, reduced signal inductance, power/ground inductance and package footprint, along with higher signal density and die shrink. A flip chip ball grid array package (FCBGA) by Texas Instruments (TI) is shown in figure 1.4.

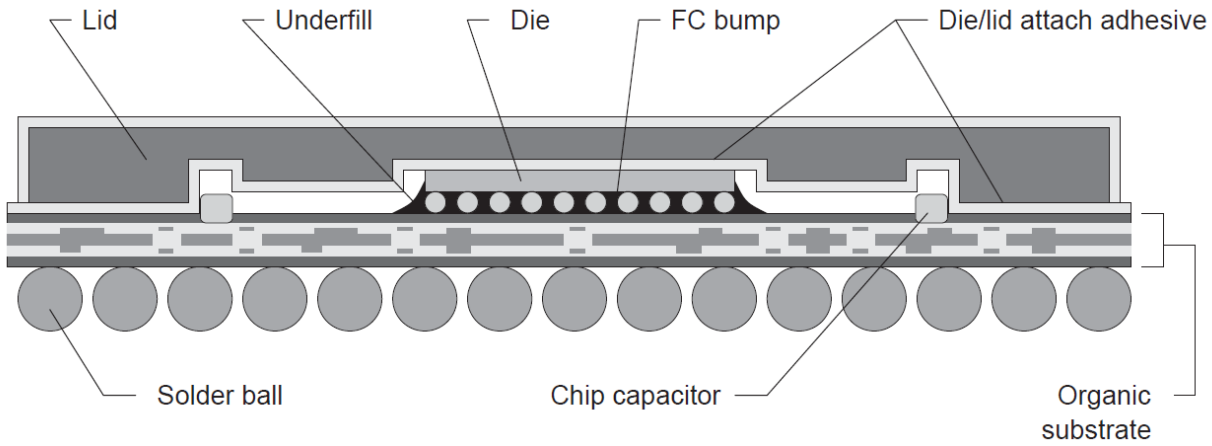

Fig. 1.4 Flip Chip Ball Grid Array Package (FCBGA) [Texas Instruments]

1.4 Power Cycling

The Phenomenon of turning OFF an electronic device and then turning it ON multiple times is knows as Power Cycling (PC). Power cycling is the more realistic and accurate prediction of fatigue life of the solder joint interconnects. Generally accelerated thermal cycling (ATC) is used to predict the life of the solder joint interconnects. The ATC assumes a uniform temperature distribution throughout the PCB assembly, which is not true. The package is subject to non-uniform distribution of temperature with the chip or die as the only source of internal heat generation. Due to this non-uniform distribution of temperature, the components having different CTE values deform differently.

1.5 Motivation and Objective

The material properties like dielectric constant, dissipation factor, moisture absorption capacity of the high frequency laminates are compared to the conventional FR-4 laminates. There is a need to assess the reliability of these high frequency laminates to recommend the use of these materials. In this work we assess the reliability of the solder joint interconnects of a BGA package on Megtron 6 and FR-4 printed circuit boards under the effect of Power cycling (PC). ANSYS Workbench 18 is used for the modeling and simulation of PC of printed circuit board assembly (PCBA). PC is applied for 3 cycles with a power density of 0.5 W/mm^3. The maximum accumulated plastic work after the end of the 3rd cycle is used for the estimation of life of the PCBA using Syed's model. Similarly, the life of Megtron 2, Megtron 4, Megtron 4s, Megtron 7 and Megtron GX is estimated and compared with Megtron 6 and FR-4.

Chapter 2

LITERATURE REVIEW

Izhar Z. Ahmed and S.B. Park [1], has discussed the fatigue life of the solder joint interconnects of a BGA package under PC and compared it with Accelerated Thermal Cycling (ATC). The author has used the CFD simulations to extract the heat transfer coefficient and imported the result to perform the subsequent thermal and structural finite element analyses (FEA) with heat generation and heat transfer coefficient as boundary conditions. The solder joint interconnects of the organic packages failed earlier under PC than ATC.

Jue Li [2], has studied the effect of PC and ATC on lead free solder interconnects of thin fine-pitch BGA both experimentally as well as Finite Element (FE) simulation. A 3-D board level FE analysis is do estimate the reliability of the solder joints under PC and ATC and the obtained results were validated experimentally. The fatigue life of the solder joint interconnects under PC is found to be longer that ATC. A study on the propagation of primary crack was also done in this work.

John Coonrod [12], compared the material properties, circuit fabrication issues, electrical performance, reliability issues, general end use considerations of the conventional FR-4 laminates with the high frequency laminates. The author has provided the guidelines to understand when to use the high frequency materials.

Mugdha Chaudari [9], in her thesis has assessed the reliability of the solder joint interconnects of a BGA package on Megtron 6 board. ATC has been performed using FEA simulation. Volume averaged plastic work has been determined as the criteria to estimate the life of the solder joint interconnect. Syed's model has been used to access the reliability. It has been found that the high frequency laminates offer higher reliability over the conventional FR-4 under ATC.

Robert Darveaux [11], has studied the factors effecting the solder joint reliability of PBGA under ATC and PC. He described the effect of change in substrate thickness, pad diameter, ramp rate and dwell time on the fatigue life of the solder joints. He found that the fatigue life of the solder joint is predicted to be 5x more under PC than ATC under some temperature profile.

Chapter 3

MATERIAL CHARACTERIZATION

It is very important to assign accurate material properties to different components of the package to obtain valid results in the FE simulations. Coefficient of thermal expansion (CTE), Glass Transition temperature (T_g) and Complex modulus (E_c) are measured through material characterization.

The Thermo-Mechanical Analyzer is used to obtain the CTE and Dynamic-Mechanical analyzer is gives the complex modulus from which the young's modulus is calculated.

3.1 Thermo-Mechanical Analyzer

3.1.1 Coefficient of Thermal Expansion (CTE)

The coefficient of thermal expansion (α) is a material property that is indicative of the extent to which a material expands upon heating. CTE may also be defined as the fractional change in length or volume of a material for a unit change in temperature.

$$\alpha = \frac{\epsilon}{\Delta T} \tag{3.1}$$

Where,

ϵ is the fractional change in length or strain (mm/mm)

ΔT is the change in Temperature (^0C)

3.1.2 Glass Transition Temperature (T_g)

The Glass Transition Temperature (T_g) is one of the most important properties of any polymer where the polymer transitions from a hard, glassy material to a soft, rubbery material. T_g is not a discrete thermodynamic transition, but a temperature range over which the mobility of the polymer chains increases significantly. The T_g of a polymer depends on the chemical structure of the resin, type of hardener and the degree of cure.

TMA consist of a quartz probe whose relative movement with change in temperature is used as a parameter to determine the CTE of the PCB material. The quartz probe is enclosed in a thermal chamber which can be operated in a wide range of temperatures. Temperatures as low as -65^{0}C can be achieved using a cooling attachment. The TMA with the cooling attachment is shown in the figure 3.1. PCB samples for the TMA with dimensions 8mm X 8mm are cut using a high-speed cutter. The TMA samples are shown in the figure 3.2. The TMA samples are subjected to a temperature range of -65^{0}C to 260^{0}C with a ramp rate of 5^{0}C/min. The start and end load applied is 100mN. The in-plane and out of plane CTE are measured using the TMA by changing the position of the PCB sample.

Figure 3.1: Thermo-Mechanical Analyzer (TMA-S6600)

Figure 3.2: 8mm X 8mm TMA sample

The figure 3.3 shows the plot for the in-plane of the Megtron 6 and the FR-4 samples. The figure 3.4 shows the out of plane CTE of the PCB samples. A significant change in slope is observed in the plots after 150^{0}C which is due to the recrystallization and cold crystallization of the samples during the experiment. The glass transition range of the samples is the region where the change of slope in the CTE plots is observed. Further expansion of the sample is observed above 180^{0}C and the melting process takes place at about 225^{0}C with the reduction in sample dimensions and viscosity.

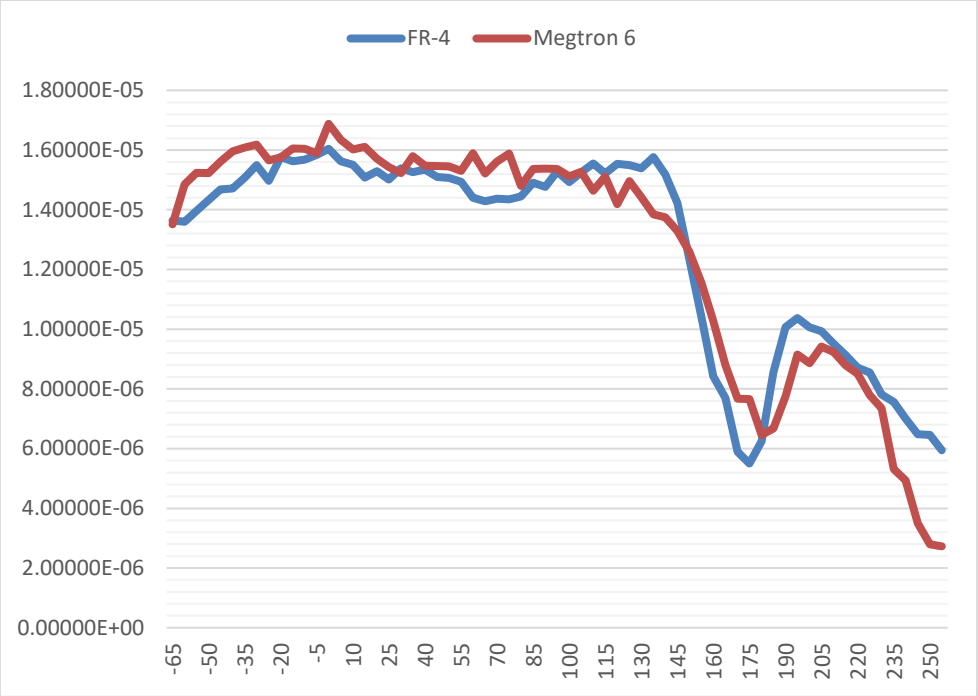

Figure 3.3: Plot for In-Plane CTE

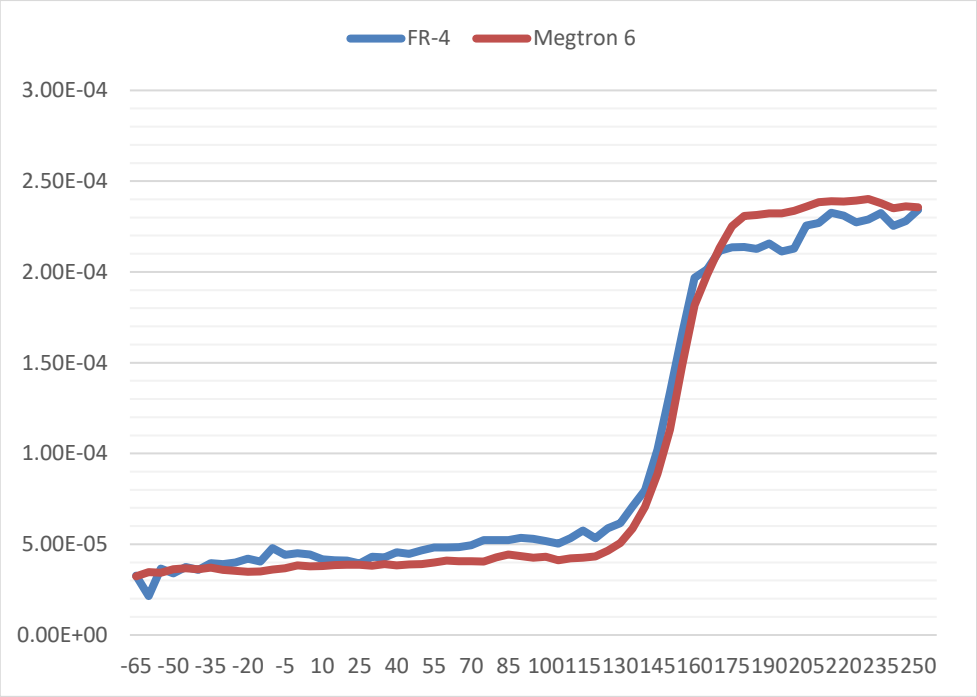

Figure 3.4: Plot for Out of Plane CTE

The table 3.1 shows the CTE values of the PCB materials in 3 directions (FR-4 and Megtron 6 used in the study. The table 3.2 shows the CTE values of other components of the PCBA obtained from the literature.

Boards	CTE(ppm/^{0}C)		
	X-direction	Y-direction	Z-direction
FR-4	15.3	13.1	41.1
Megtron 6	15.39	13.2	43.1

Table. 3.1 CTE measured using TMA

Material	CTE(ppm/^{0}C)
Copper Pad	17.78
Die Attach	65
Die	2.94
Mold	8.43
Polyimide Layer	35
Solder Mask	30

Table. 3.2 CTE of other components

3.2 Dynamic Mechanical Analyzer

3.2.1 Storage Modulus (E')

The storage modulus is the measure of energy stored, representing the elastic portion of a material. Figure 3.5 shows the storage modulus with change in temperature of Megtron 6 measured using the DMA.

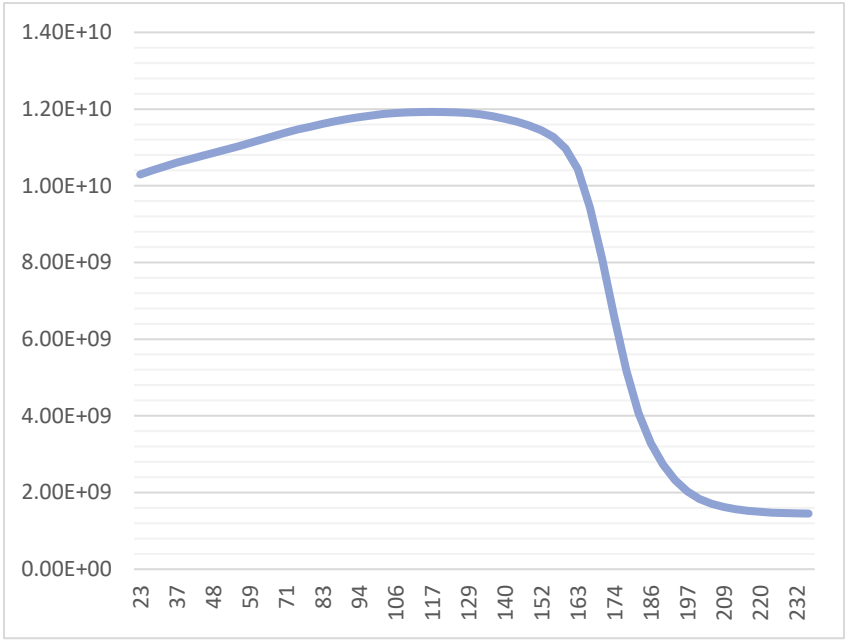

Figure 3.5: Plot for Storage Modulus

3.2.2 Loss Modulus (E'')

The Loss Modulus is the measure of energy dissipated as heat, representing the viscous portion of the material. Figure 3.6 shows the change in loss modulus of Megtron 6 with change in temperature.

3.2.3 Complex Modulus (E_c)

The complex modulus is a complex number whose real part is storage modulus (E') and the imaginary part is the loss modulus (E''). It is given by (3.2)

$$E_c = (E') + i\,(E'') \qquad (3.2)$$

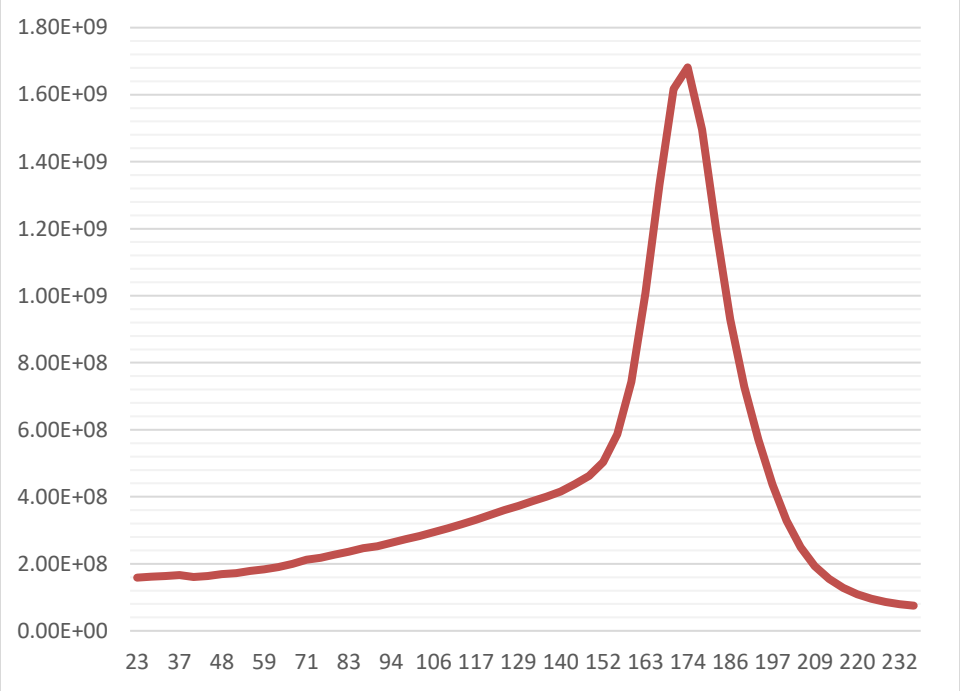

Figure 3.6: Plot for Loss Modulus

3.3.3 Young's Modulus (E)

Young's modulus is the elastic modulus used to calculate the deformation of a material which takes place when a force parallel to the axis of the object is applied to one face which the opposite face is held fixed by another equal force. It is also called as Tensile Modulus or Modulus of Elasticity or Elastic Modulus. It is a measure of stiffness of the PCB. The argument of the complex modulus (E_c) is the measure of the Young's Modulus (E).

$$|E_c| = E = \sqrt{(E')^2_+(E'')^2} \qquad (3.3)$$

The Dynamic Mechanical Analyzer (DMA) is used to measure the complex modulus (E_c), using which the Young's modulus (E) of the PCB material is calculated. The PCB sample of dimensions 50mm X 10mm in length and width, shown in figure 3.5, is clamped in a bending apparatus. Care should be taken that the sample is doesn't gets displaced during the experiment. A sinusoidal wave is generated using a force motor which transmits it to the sample through a drive shaft. This applies a cyclic load due to which the sample is deformed.

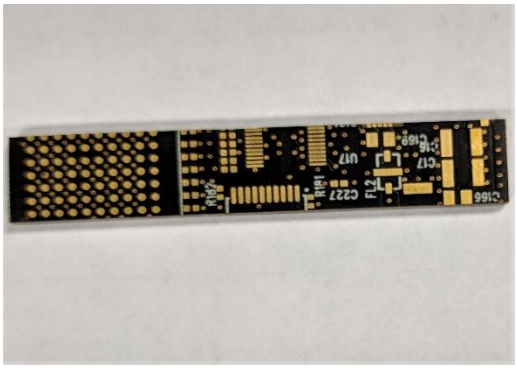

Figure 3.7: 50mm X 10mm DMA Sample

Table 3.3 show the calculated values of Young's modulus and Poisson's ration of Megtron 6 and FR-4 boards. Table 3.4 shows the Young's modulus values of the other components of the PCBA obtained through literature review. Table 3.5 shows the material properties of other PCB boards in the Megtron series considered in this study.

Material	Young's Modulus (GPa)	Poisson's Ratio
FR-4	15.46	0.39
Megtron 6	13.8	0.2

Table 3.3 Young's Modulus and Poisson's Ratio of FR-4 and Megtron 6

Material	Young's Modulus (GPa)
Copper Pad	110
Die Attach	154
Die	150
Mold	24
Polyimide Layer	3.3
Solder Mask	4.6

Table 3.4 Young's Modulus and Poisson's Ratio of Other Components

Boards	CTE(ppm/^{0}C)			E(GPa)	υ
	X-direction	Y-direction	Z-direction		
Megtron 2	15	15	34	16.7	0.2
Megtron 4	14.5	14.5	35	15.9	0.2
Megtron 4s	14	14	32	15.1	0.2
Megtron 7	16	16	42	13.5	0.2
Megtron GX	10	10	22	29	0.2

Table 3.5. Material Properties of Megtron Series Boards

Chapter 4

MODELING AND SIMULATION

4.1 Introduction to Finite Element Analysis (FEA)

Finite element procedures are numerical method for solving a problem, now important and necessary part of engineering design and analysis. FE procedures are very extensively used in the analysis of solids and structures and of heat transfer, fluids and are virtually being employed in all the fields of engineering analysis. In the FE analysis the model body is divided into many smaller elements or units called the finite elements, are interconnected at common points of two or more elements. This common point is called a node or nodal point. This process of division of the model body into elements is called discretization. Then a set of governing algebraic equations are developed and solved under certain assumptions. There exists a governing equation for each element. All these equations are combined to obtain the solution of the model body.

Since the FE analysis is a numerical procedure, there is always a necessary to check the accuracy of the obtained solution. If the required accuracy conditions are not met, the solution must be repeated with refined parameters such as using finer mesh or a different type of element until an acceptable solution is obtained. The analysis of the structural problems deals with determining the nodal displacements, stresses and strains associated with each element under the applied loading conditions. The governing equation to determine the nodal displacement using FE techniques is given by (4.1)

$$[F] = [K]\{u\} \qquad (4.1)$$

[F] is a column matrix which represents the force vector which depends on the boundary conditions and applied loading conditions, [K] is a symmetric matrix which is the global stiffness matrix which depends on the material properties and geometry of the object, {u} is a column matrix which represents the nodal displacement.

A typical FE analysis consists of 3 steps:

1. Preprocessing, which is divided into 3 sub steps
    - Modeling the geometry.
    - Assigning the material properties.
    - Mesh generation.

2. Solution, which is divided into 4 sub steps
    - Application of loads and boundary conditions.
    - Selection of output and load step controls.
    - Selection of solver.
    - Obtaining the solution.
3. Post Processing
    - Review the obtained results.

In this study few assumptions are made while creating the geometry. They are as follows:

1. The PCB is Orthotropic.
2. All the materials except the solder balls are considered as linearly elastic.
3. The solder is modeled as rate dependent viscoplastic material using Anand's Viscoplastic model.

4.2 Geometry

A silicon die, which is enclosed in a mold is attached to the substrate solder mask using a die attach. The substrate solder mask is further attached to the polyimide layer. The package has copper pads on both top and bottom sides of the solder balls. The cross section of the BGA package modeled in this study is shown in the figure 4.1.

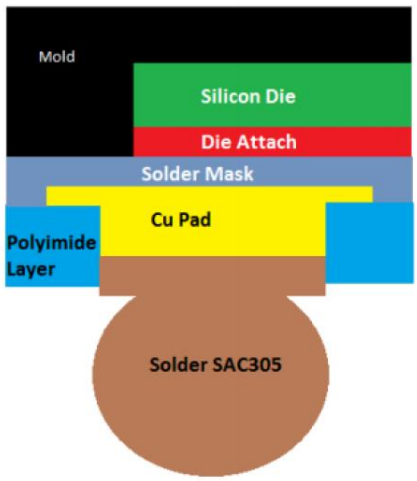

Figure 4.1: Cross-Section of the BGA package

The FR-4 board used in the study has 8 layers (1-6-1) of copper where as the Megtron 6 has 18 layers (1-16-1). Both the boards have same thickness of approximately 2mm. A 11 X 11 array Micro star BGA is modeled in ANSYS 18. Table 4.1 shows the dimensions of the package. The schematic of the BGA is shown in the figure 4.2.

Component	Dimensions (mm)
Package	6 x 6 x 0.74
Die	4.5 x 4.5 x 0.28
Solder ball pitch	0.5
Solder ball diameter	0.3
Solder ball height	0.2
Solder mask thickness	0.05
Substrate thickness	0.05
Copper pad thickness	0.04

Table 4.1 Package Dimensions

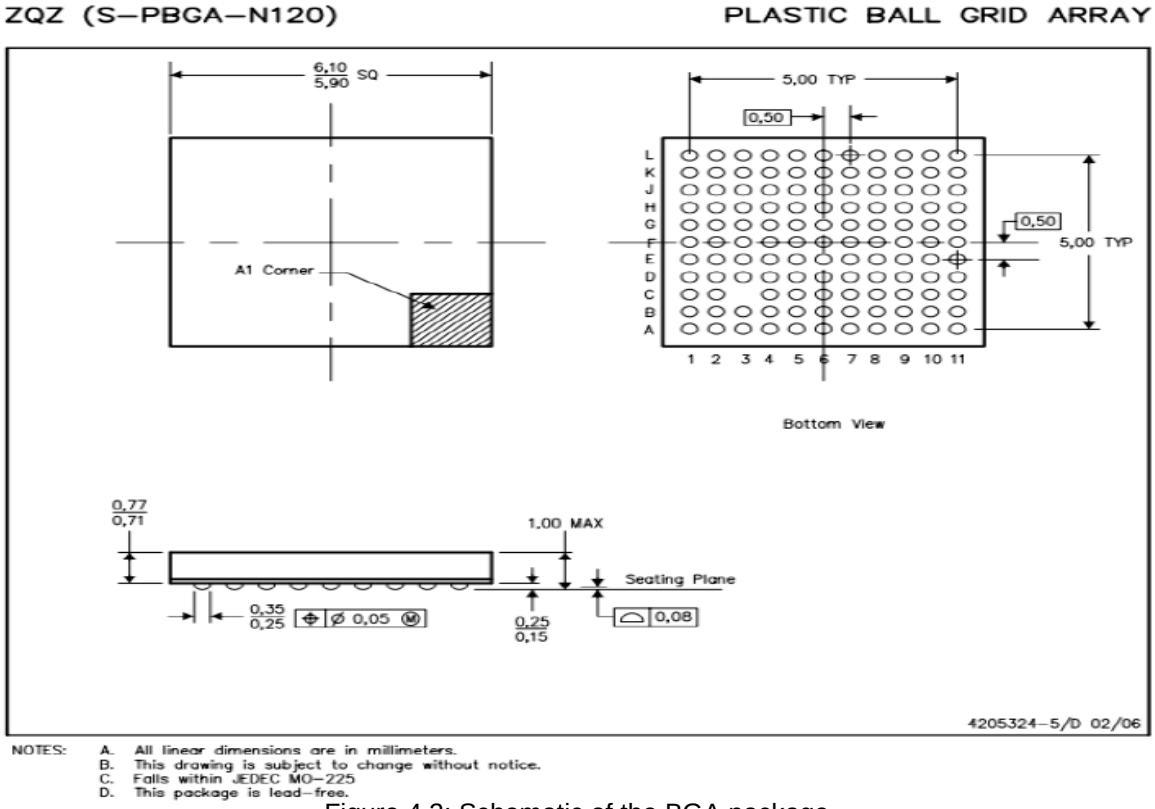

Figure 4.2: Schematic of the BGA package

An octant symmetry model is considered for the analysis. Figure 4.3 show the octant symmetry model. The figure 4.4 show the cross-section of the package modeled in ANSYS.

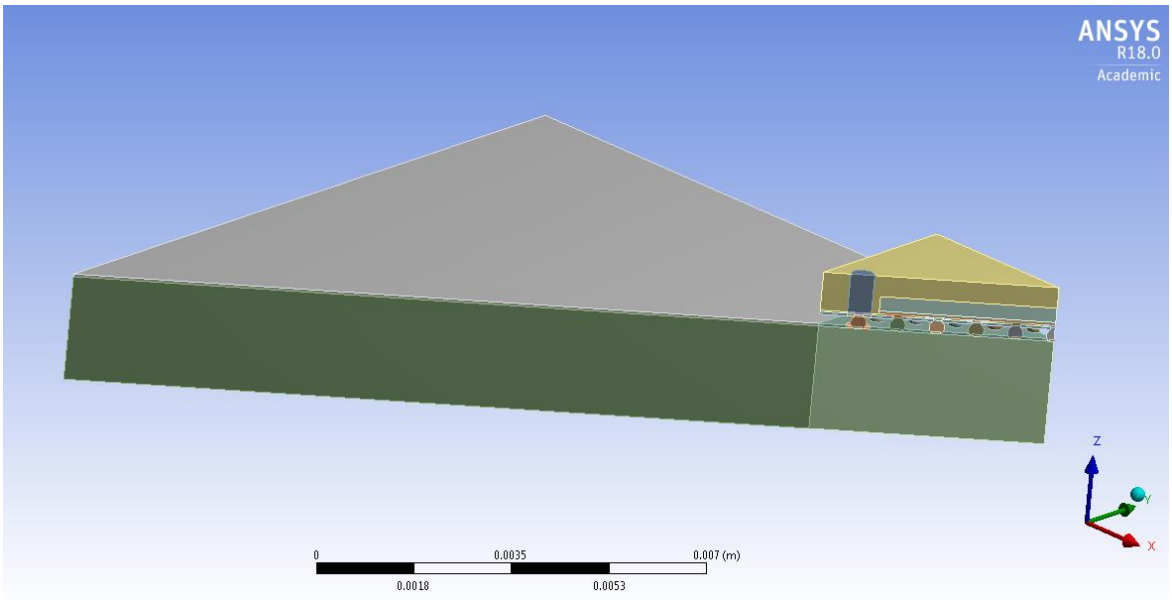

Fig. 4.3 Octant Symmetry Model

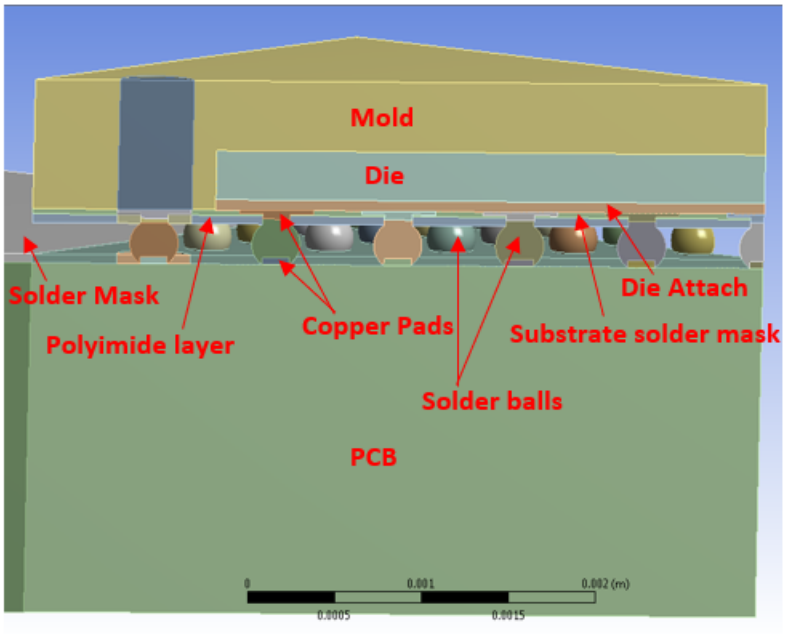

Fig. 4.4 Cross-Section of Geometry

4.3 Material Properties

As already mentioned in the assumptions, the package is considered linearly elastic, PCB is orthotropic, and the solder ball is a rate dependent viscoplastic material modeled based on Anand's

viscoplastic law. The material properties determined during the material characterization are used. The input is given for the temperature dependent CTE, Young's modulus, Poisson's ratio and temperature dependent shear modulus. The solder all used is SAC305 whose composition is 96.5% Tin(Sn), 3% Silver(Ag) and 0.5% Copper(Cu). Using Anand's viscoplastic model both plastic deformation and creep are considered to represent the secondary creep of the solder.

The total strain is given by (4.2)

$$\epsilon_{ij} = \epsilon_{ij}^{e} + \epsilon_{ij}^{in} \tag{4.2}$$

Where ϵ_{ij}^{in} is the inelastic strain tensor.

Anand's viscoplastic model, the inelastic strain rate is coupled to the rate of deformation resistance.

The equation (4.3) gives the strain rate

$$\frac{d\varepsilon_{in}}{dt} = A\left[\sin h\left(\xi\frac{\sigma}{s}\right)\right]^{\frac{1}{m}} \exp\left(-\frac{Q}{RT}\right) \tag{4.3}$$

The rate deformation resistance is given by

$$\dot{s} = \left\{h_0(|B|)^{\alpha}\frac{B}{|B|}\right\}\frac{d\varepsilon_p}{dt} \tag{4.3}$$

$$B = 1 - \frac{s}{s^*}$$

$$s^* = \hat{s}\left[\frac{1}{A}\frac{d\varepsilon_p}{dt}\exp\left(-\frac{Q}{RT}\right)\right]$$

Where $\frac{d\epsilon_{in}}{dt}$ is the effective inelastic strain rate, σ is the effective true stress, *s* is the deformation resistance, T is the absolute temperature, A is pre-exponential factor, ξ is stress multiplier, m is the strain rate sensitivity of stress, Q is activation energy, R is universal gas constant, h_0 is hardening/softening constant, $\hat{s}$ is coefficient for deformation resistance saturation value, *n* is strain-rate sensitivity of saturation value, and *a* is strain rate sensitivity of hardening or softening. The nine material constants of Anand's viscoplastic law are listed in the table 4.2.

Constant	Name	Unit	Value
s0	Initial Deformation Resistance	MPa	12.41
Q/R	Activation Energy/ Universal Gas Constant	1/K	9400
A	Pre- exponential Factor	sec^{-1}	4E+06
ξ	Multiplier of Stress	Dimensionless	1.5
m	Strain Rate Sensitivity of Stress	Dimensionless	0.303
h0	Hardening/Softening Constant	MPa	1378.8
ŝ	Coefficient of Deformation Resistance Saturation	MPa	0.07
n	Strain Rate Sensitivity of Saturation	Dimensionless	1.3
a	Strain Rate of Sensitivity of Hardening or Softening	Dimensionless	1.6832

Table 4.2 Anand's constants for SAC305

4.4 Meshing

Hex dominant meshing and three node elements are used for the solder balls. The critical solder is determined to the farthest from neutral point (midpoint of the package). Different body sizing has been used for each component of the PCB assembly to get accurate results. Figure 4.5 (a) shows the meshed octant model and figure 4.5 (b) show the meshed solder balls. Table 4.2 shows the body sizing of the different components.

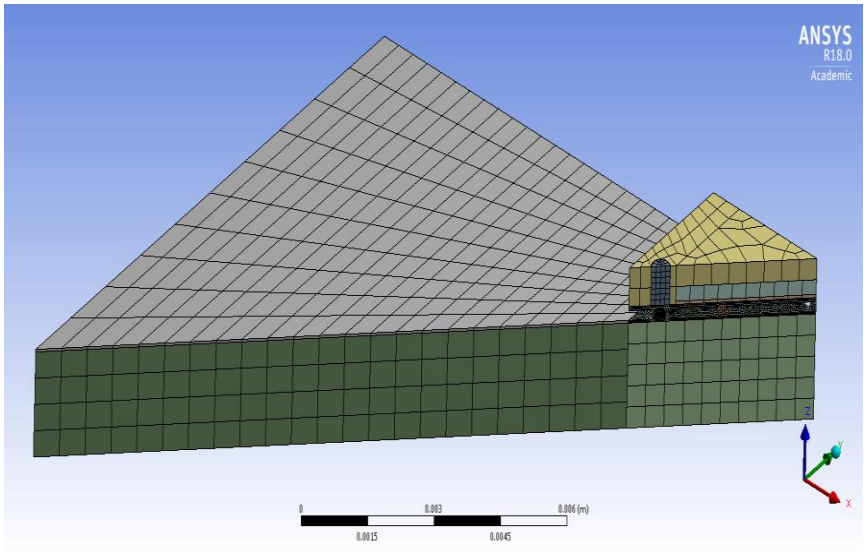

Figure 4.5 (a): Meshed Octant Symmetry Model

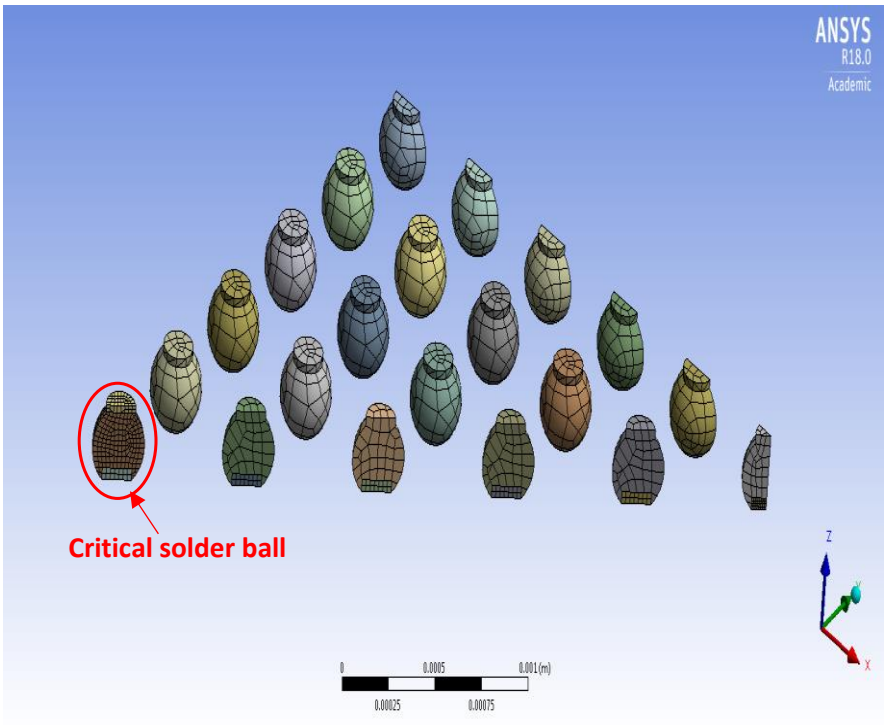

Figure 4.5 (b): Meshed Solder balls

Component	Body Sizing(m)
Critical Solder ball	2E-5
Other solder balls	9E-4
Copper pads (package side)	5E-5
Copper pads (board side)	9E-4
Substrate layer	5E-5
Solder mask	5E-5
PCB below the package	9E-4
PCB	5E-4

Table 4.3 Body sizing of different components

4.5 Loading and Boundary conditions

Transient structural analysis is to be conducted to obtain the desired results. The model is created, and the required material properties are assigned. The transient thermal analysis gives the temperature attained by the package when the die emits heat. The obtained temperature results are imported to the static structural module to do the further analysis and obtain the plastic work which is used as a parameter to estimate the life of the solder balls.

4.5.1 Boundary Conditions

In the transient thermal analysis, convection boundary conditions is applied to all the faces of the package that is exposed to the environment. A convective heat transfer co-efficient of 23 $W/m^2\ ^0C$ is given [1]. Figure 4.6 show the convective faces of the PCB assembly. In the static structural analysis, friction less supports are applied on the faces of symmetry of the PCB assembly and the common of the package is fixed. Figure 4.7 shows the structural boundary conditions.

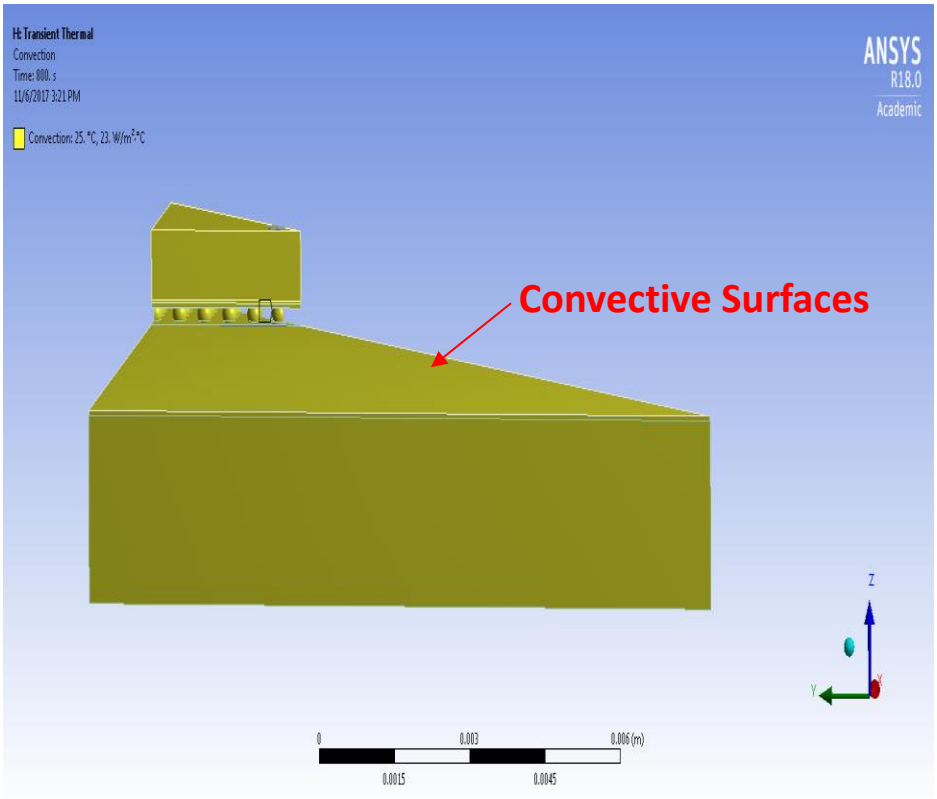

Figure 4.6: Convection Boundary Condition

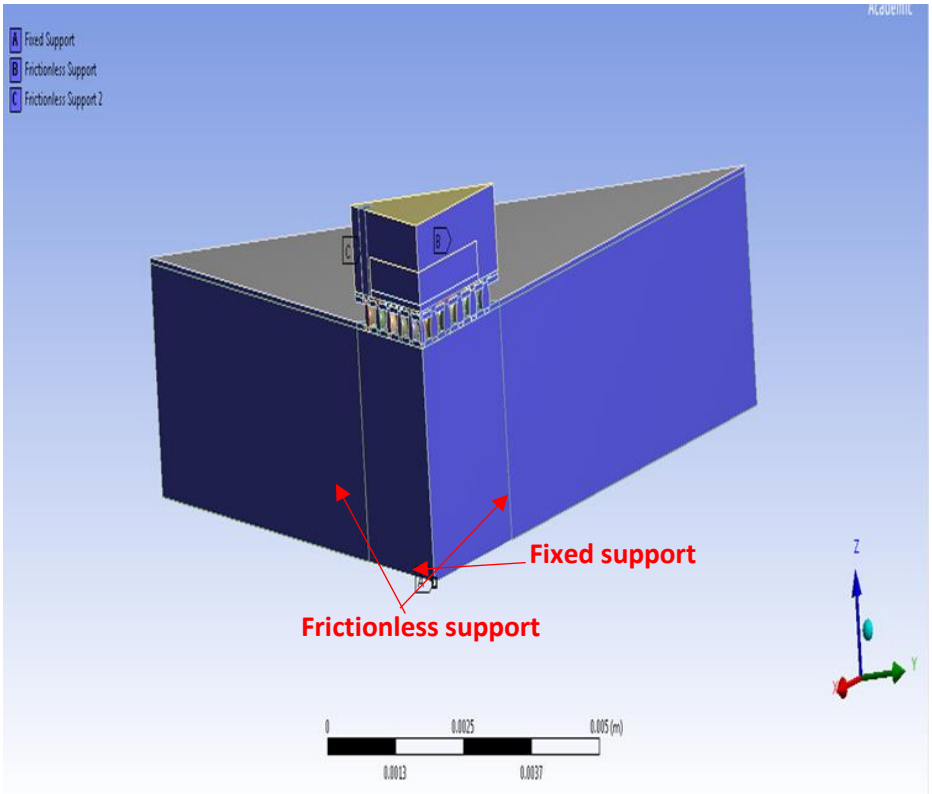

Figure 4.7: Structural Boundary Conditions

4.5.2 Loading Conditions

In the power cycling analysis, the die or chip is the only source of power generation. 3 cycles of a very low power density of 0.5 W/mm^3 is applied with a total cycle time of 1600 seconds which comprises of 800 seconds ON and 800 seconds OFF. The figure 4.8 shows the plot for power cycling with time on the horizontal axis and power density on the vertical axis.

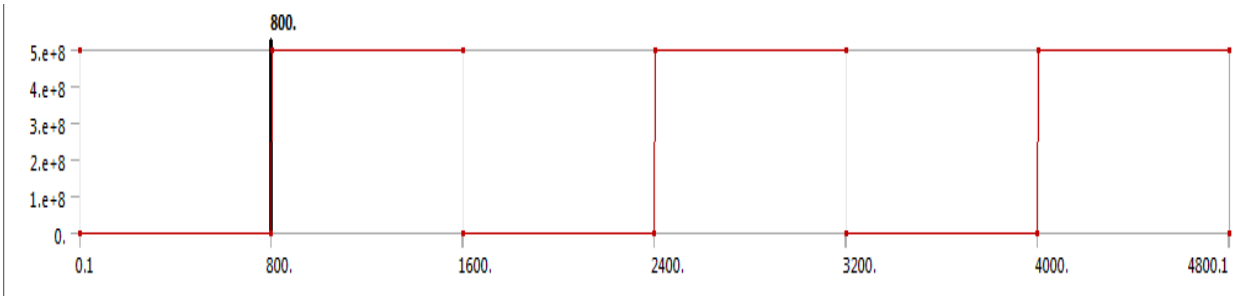

Figure 4.8: Plot for Power Cycling (PC)

Chapter 5

FATIGUE LIFE PREDICTION MODEL

5.1 Introduction

The fatigue life prediction model is used to estimate the number of cycles to failure of a package. The life of the package is usually between 100 to 10,000 cycles. The fatigue damage parameters like Creep, Plastic strain range and Accumulated plastic work causes the thermos mechanical failure of the solder joint interconnects. In this study, the maximum accumulated plastic work is used as the criteria for failure. Syed's Model is used to predict the number of cycles to failure which is given by equation (5.1).

$$N_f = 674.08\ (\Delta W)^{-0.9229} \qquad (5.1)$$

Where, N_f is the cycles to failure

ΔW is the change in plastic work in MPa

The figure 5.1 shows the plot for change in mean life of the package with accumulated creep strain energy density per cycle. Syed used a SnAgCu solder for the life prediction of CSP and BGA packages.

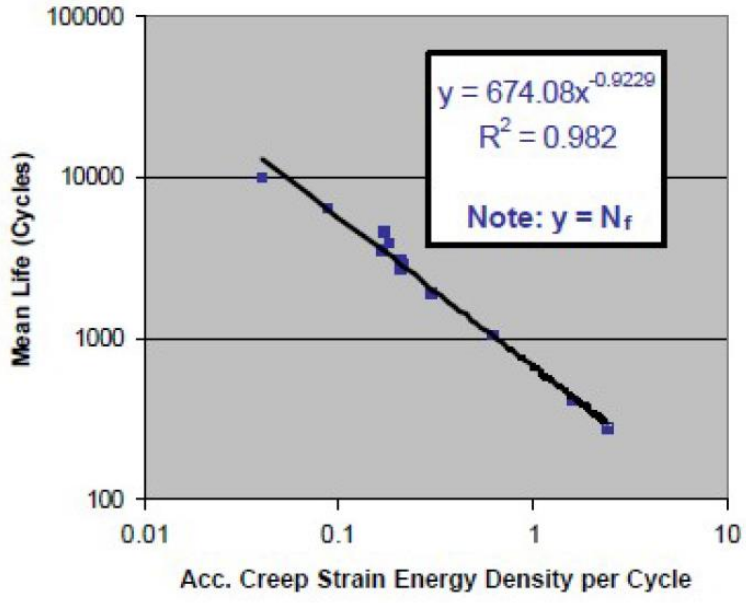

Figure 5.1: Plot showing change in Mean life with change in Accumulated Creep Strain Energy Density per Cycle

The inelastic strain energy density, also called accumulated plastic work is the area under the stress- strain loop. The comparison between the inelastic dissipate energy and the elastic strain density is shown by figure 5.2, the cyclic stress-strain hysteresis loop.

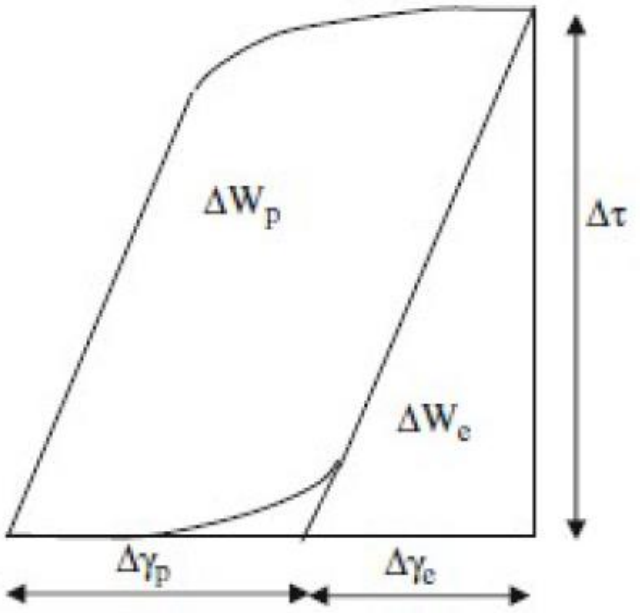

Figure 5.2: Cyclic Stress-Strain Hysteresis loop.

Chapter 6

RESULTS AND CONCLUSION

6.1 Transient Thermal Analysis

6.1.1 Temperature Distribution

As discussed earlier, power cycling is a more realistic phenomenon and there exists a non-uniform temperature distribution in the package when the device is turned on i.e., the chip or die is emitting the heat. The figure 6.1 show the distribution of temperature in the package when 3 power cycles are simulated with a power density of 0.5 W/mm^3, with the die as the heat emitting source.

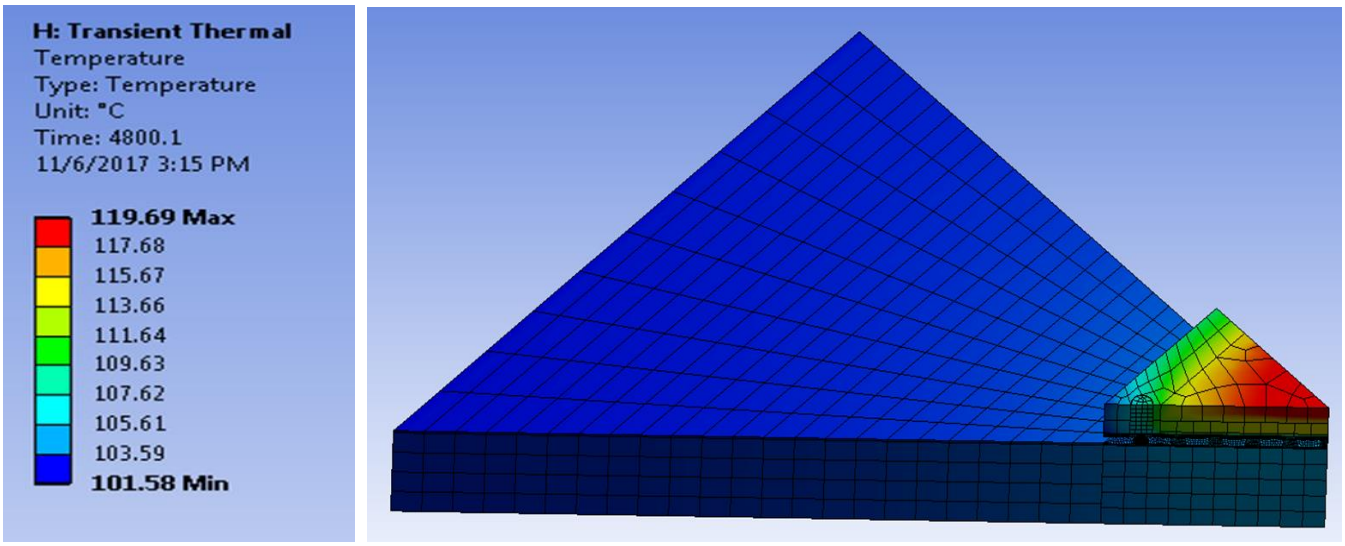

Figure 6.1: Temperature distribution in the package.

The maximum temperature attained by the package is 119.69 ^{0}C and the minimum temperature of the package is 101.58 ^{0}C. The figure 6.2 shows the plot for variation of temperature in each cycle.

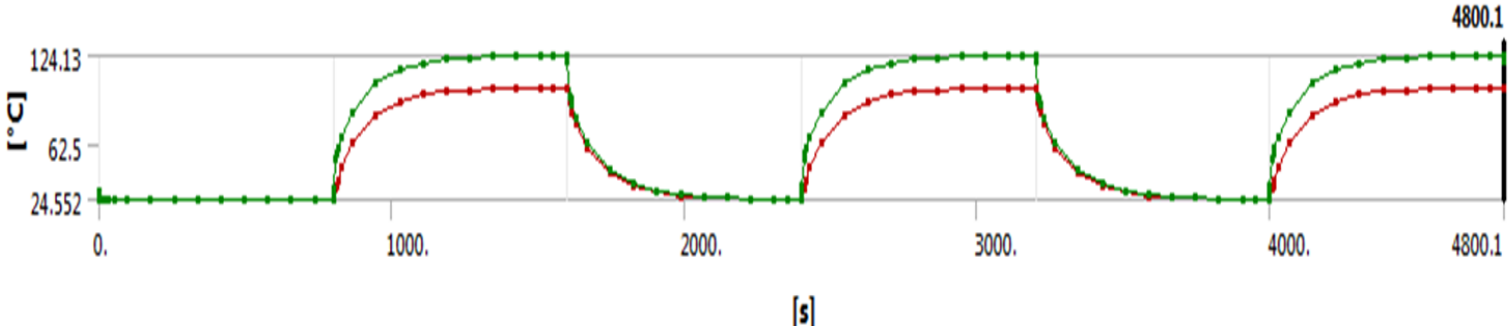

Figure 6.2: Plot Showing the Temperature Profile

The temperature distribution in the package is obtained through the transient thermal analysis. This non-uniform temperature distribution is imported to the static structural module to carry out the static structural analysis to determine the failure parameters of the package.

6.2 Static Structural Analysis

By performing the structural analysis, it is found that the solder ball at greater distance from the neutral point fails. It is observed that the failure of the solder ball occurs on the package side. The figure 6.3 show the array of solder balls with maximum stress on the corner solder balls.

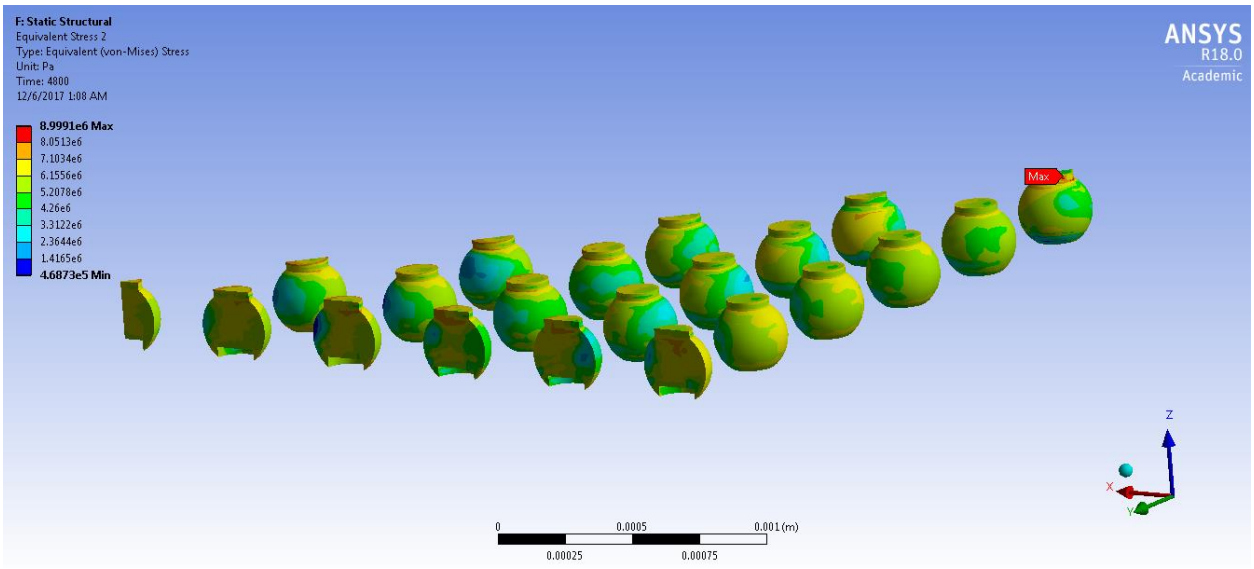

Figure 6.3: Maximum stress on the package side of the corner solder ball

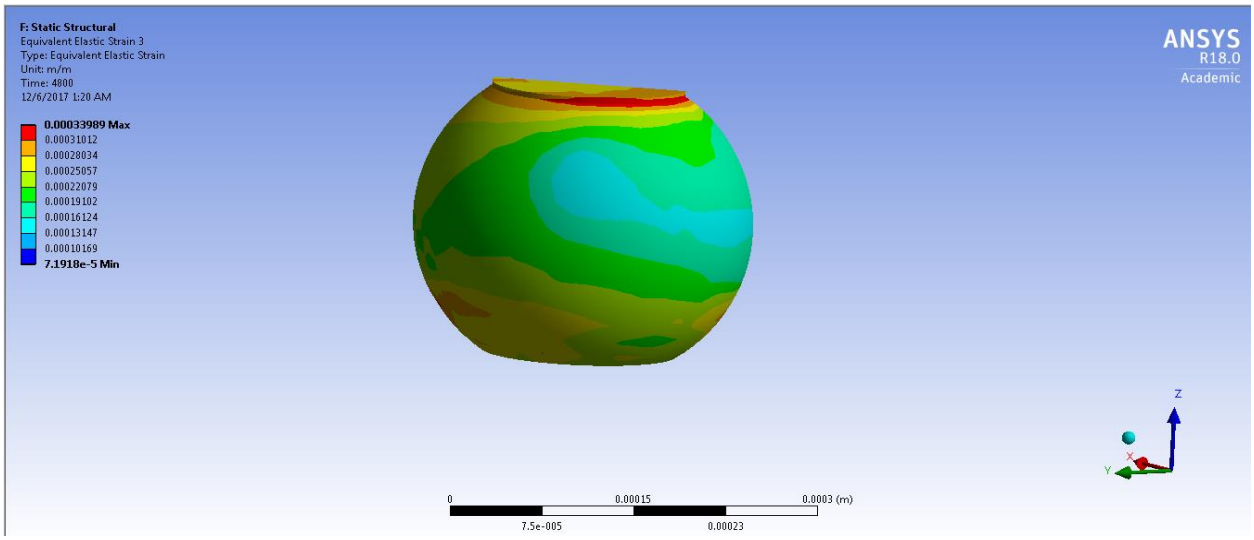

Figure 6.4: Maximum Elastic strain on the package side of corner solder ball

6.2.1 Total Deformation

The maximum deformation is observed on the corner solder ball on the package side. The figure 6.4 shows the plot for comparison maximum deformation for the FR-4 and the Megtron series boards. The solder ball on the FR-4 board deform the most where as Megtron 4s shows the least deformation.

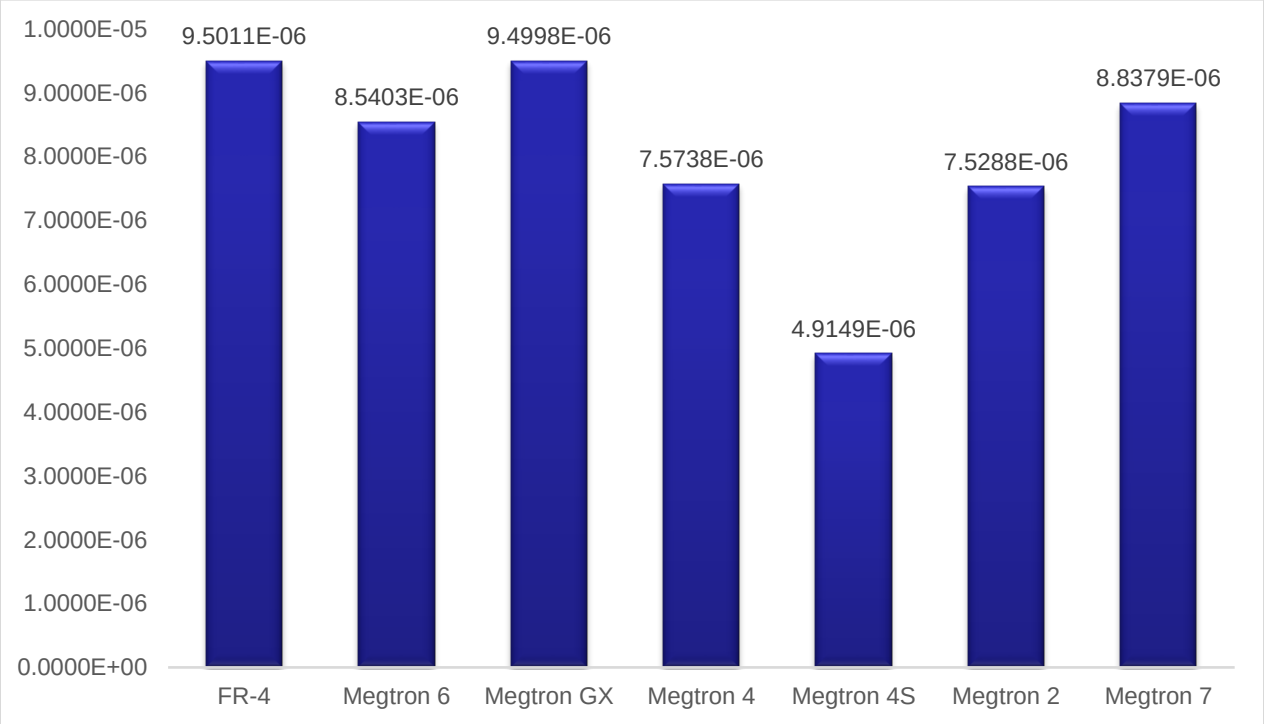

Figure 6.5: Plot for Total Deformation of the Corner Solder Ball

6.2.2 Equivalent Strain

The maximum equivalent strain is observed on the corner solder ball. The equivalent strain comparison for the Megtron series and FR-4 is shown in the figure 6.5. The strain in the Megtron 6 is less than FR-4. This shows that the FR-4 board is stiffer than the Megtron 6.

6.2.3 Maximum Accumulated Plastic Work

The maximum accumulate plastic work is used as the parameter to estimate the life of the solder joint interconnects. Since the solder ball is not flexible and will continue to deform it which eventually fails by cracking, the calculation of plastic work is of greater importance. The solder ball fails due to the mismatch in the CTE of the package and the PCB. It is more logical to consider the maximum accumulated plastic work per cycle instead of change in the maximum accumulated volume averaged plastic work because the

latter may overestimate the life of the package [1]. The figure 6.6 shows the comparison of maximum accumulated plastic work per cycle of Megtron series and FR-4 boards.

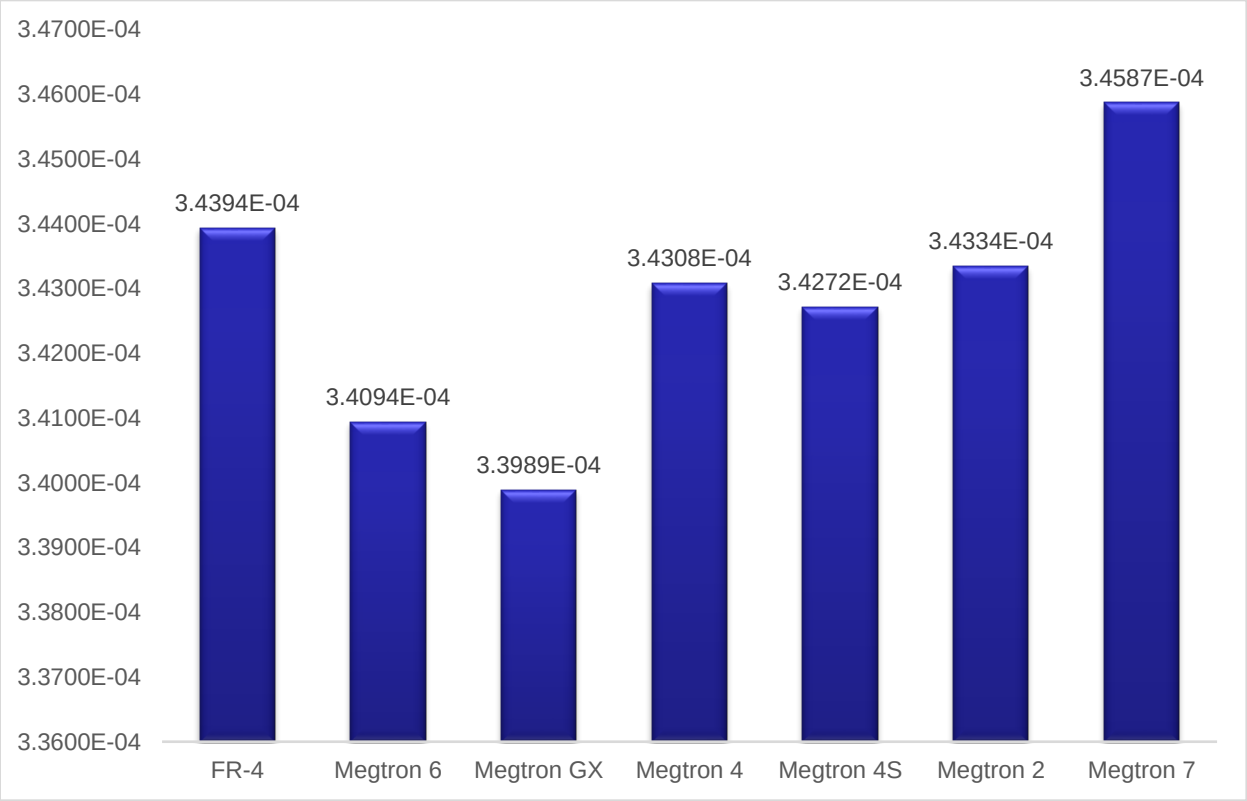

Figure 6.6: Plot for Elastic Strain on Corner Solder Ball

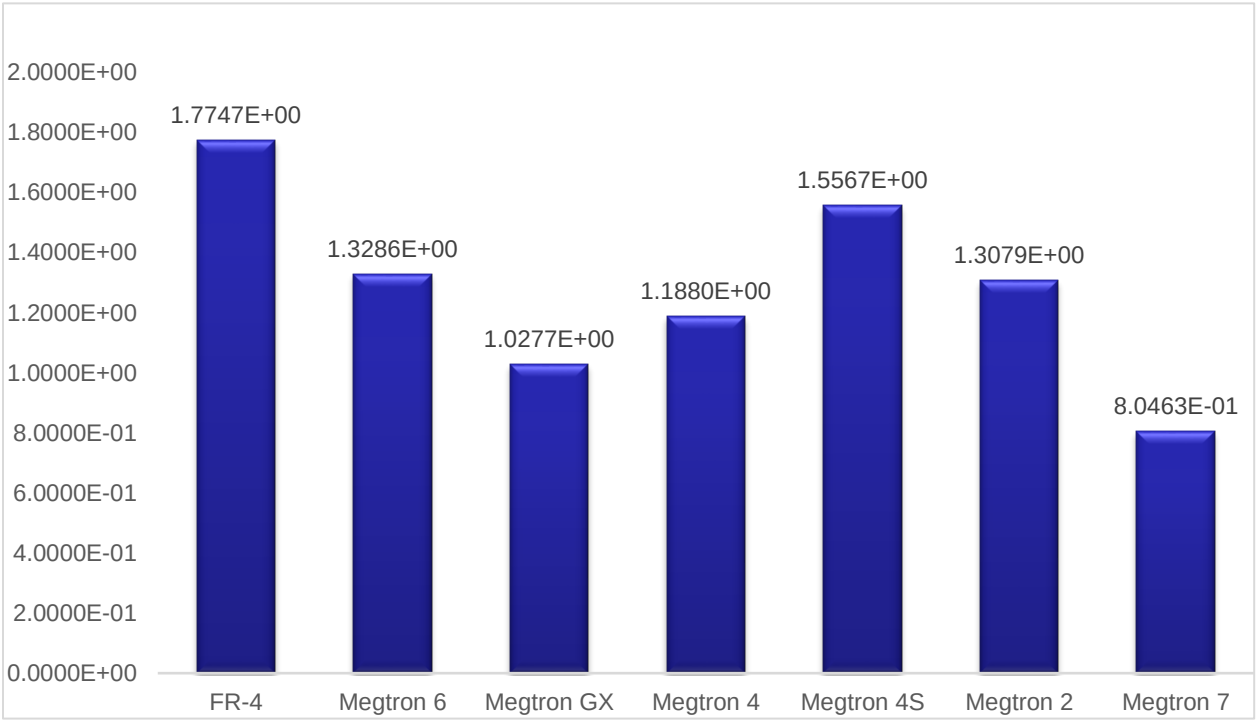

Figure 6.7: Plot for Maximum Accumulate Plastic Work per Cycle(MPa)

It is observed that the FR-4 have maximum accumulate plastic work per cycle when compared to all the boards in the Megtron series. The Megtron 6 board has 25% less accumulated plastic work than the FR-4 board. The least accumulate plastic work is seen for the Megtron 7.

6.2.4 Cycles to Failure

Syed's Model is used to calculate the cycles to failure. As mentioned in the above section, ΔW in the equation 5.1 is replaced by maximum accumulated plastic work per cycle. Figure 6.7 show the plot for cycles to failure. Megtron 6 is found to be more durable than the conventional FR-4 board by 30.73%. Megtron 7 has highest life with 823 cycles to failure under the power cycling conditions.

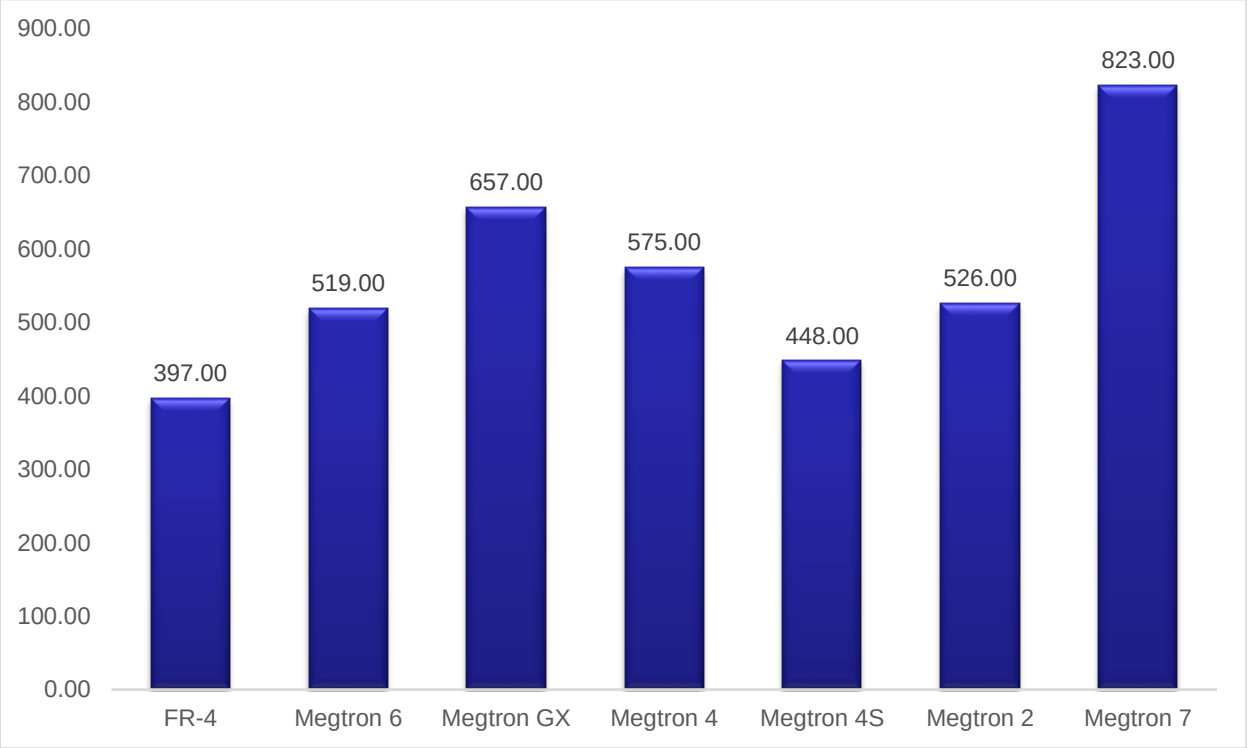

Figure 6.8: Plot for Number of Cycles to Failure

6.3 Conclusion

The material characterization was successfully performed to calculate the coefficient of thermal expansion (CTE) using the TMA and the complex modulus (E_c), which is used to calculate the Young's modulus (E) of the PCB using the DMA. The BGA package is modeled in ANSYS and the results were analyses for the total deformation, maximum equivalent strain and maximum accumulated plastic work per cycle is calculated using the Finite Element Analysis. The failure was observed on the corner solder ball

which is at the farthest distance from the neutral point (DNP) on the package side. The reliability of the Megtron 6 board is compared with the conventional FR-4 board as well as the other boards in the Megtron series. It was observed that the total deformation of the Megtron 6 is 10.11% less than FR-4. Megtron 4s has the least total deformation. Equivalent strain on the critical solder ball of Megtron 6 is less than FR-4. The Megtron 6 is found to be more durable than the FR-4 board by 30.73%, while Megtron 7 has highest life to failure under the power cycling conditions. Since, the decomposition temperature of the Megtron 6 is 410^0C is can be used in the high temperature applications. Low dielectric constant, low dissipation factor, low moisture absorption capacity, better impedance control, better thermal management are other favorable factors of the Megtron series boards when compared to the FR-4 laminates.

6.4 Future Work

The power cycling can be performed experimentally to validate the obtained simulated results. A detailed layer by layer can be modeled and analyzed to access the reliability of the package. A study on effect of underfill material on the reliability of the large packages using the high-speed laminates can be performed. Propagation of crack in the solder ball a high-speed laminate can be studies.

REFERENCE

[1] Izhar Z. Ahmed, S.B. Park "*An Accurate Assessment of Interconnect Fatigue Life Through Power Cycling*", IEEE, Inter Society Conference on Thermal Phenomena 2004.

[2] Jue Li, Juha Karppinen, Tomi Laurila and Jorma Kalevi Kivilahti, "*Reliability of Lead-Free Solder Interconnections in Thermal and Power Cycling Tests*", IEEE Transactions on Components and Packaging Technologies 2009.

[3] Diane E. Hodges Popps, Andrew Mawer and Gabriel Presas, "*Flip Chip PBGA Solder Joint Reliability: Power Cycling versus Thermal Cycling.*"

[4] Werner Engelmaier, "*Fatigue Life of Leadless Chip Carrier Solder Joints During Power Cycling*", IEEE Transactions on Components, Hybrids and Manufacturing Technology 1983.

[5] Andrew Eugene Perkins, "*Investigation and Prediction of Solder Joint Reliability For Ceramic Area Array Packages Under Thermal Cycling, Power Cycling and Vibration Environments*", Thesis, Georgia Institute of Technology.

[6] Brayn Rodgers, Jeff Punch and John Jarvis "*Finite Element Modeling of a BGA Package Subjected to Thermal And Power Cycling*", IEEE, Inter Society Conference on Thermal Phenomena 2002.

[7] Tong Yan Tee, Hun Shen Shen Ng, Zhaowei Zhong and Jiang Zhou, "*Board-Level Solder Joint Reliability Analysis of Thermally Enhanced BGA and LGA's*", IEEE Transactions on Advanced Packaging 2006.

[8] Liulu Jiang, Wenhui Zhu, Hu He, "*Comparison of Darveaux Model and Coffin-Manson Model for Fatigue Life Prediction of BGA Solder Joints*" IEEE, 18th International Conference on Electronic Packaging Technology 2017.

[9] Mugdha Anish Chaudhari "*Reliability Assessment of Solder Joint Using BGA Package-Megton 6 Versus FR-4 Printed Circuit Board*", Masters Thesis, The University of Texas at Arlington 2017.

[10] Unique Ranhangdale, B. Conjeevaram, Aniruddha Doiphode, Pavan Rajmane, Abel Misrak, A.R. Sakib, Dereje Agonafer "*Solder ball Reliability Assessment of WLCSP- Power cycling versus Thermal Cycling*" ITHERM 2017.

[11] Robert Darveaux and Andrew Mawer, “Thermal and Power Cycling Limits of Plastic Ball Grid- Array (PGBA) Assemblies”, SMTA Surface Mount International 1995

[12] John Coonrod, “*Understanding When to use FR-4 Or High Frequency Laminates*”, Onboard Technology September 2011

[13] Texas Instruments, “*Flip Chip Ball Grid Array Package Reference Guide.*”

[14] Sumanth Krishnamurthy, “*Experimental and Computational Board Level Reliability Assessment of Thich Board QFN Assemblies Under Power Cycling*” Masters Thesis, The University of Texas at Arlington 2016.

BIOGRAPHICAL INFORMATION

Mahesh Pallapothu pursued his bachelor's degree (Bachelor of Technology) in Mechanical Engineering at Jawaharlal Nehru Technological University, Hyderabad in 2015. He moved to the United States in 2016 for his master's degree in Mechanical Engineering at The University of Texas at Arlington. He was an active member of EMNSPC reliability team and was the Event officer of the Surface Mount Technology Association Student Chapter at the University of Texas at Arlington. He was a recipient of Kelcy Warren Fellowship award for the academic year 2016-2017. His research includes experimental material characterization of the printed circuit boards, 3-d Modeling and thermo-mechanical simulation of the electronic package to estimate the reliability of the given package. He successfully completed his Master of Science Degree in Mechanical Engineering in Fall 2017. After graduation he plans to start his professional career in the field of electronic packaging and semiconductors.